

# DESIGN OF LIGHTNING ARRESTERS FOR ELECTRICAL POWER SYSTEMS PROTECTION

Shehab Abdulwadood ALI

Department of Physics, College of Saber, University of Aden, 867 Street 10B, Sheikh Othman, Aden, Yemen

shehababdulwadood@gmail.com

**Abstract.** This paper presents an overview of how the lightning strikes and their effects on power distribution systems can be modeled, where the results give a clear picture of how to eliminate the devastating impact, caused by lightning, by using lightning arresters. The program ATP-Draw (Alternative Transient Program) was used to simulate the problem and was applied on a part of a power network. The simulation was done once when the lightning strikes a transmission line and a substation with no lightning arresters in use and once more with their use. The source of the lightning was represented by the ATP models (Type-15 surge function and Type-13 ramp function) and the surge arrester was represented by the MOV-Type 92 component. The voltage was recorded at the substation 110/22 kV and at all loads in the electric network, and was drawn by the PlotXWin program. The results obtained indicate that the voltages induced by the lightning can reach values of the order of millions over insulation flashover levels for 22 kV equipment, where is clearly seen in Fig. 9 to Fig. 13 and Tab. 10, which requires the installation of lightning arresters.

## Keywords

*Lightning, lightning arresters, MOV, overvoltage, residual voltage.*

## 1. Introduction

Lightning is the most frequent cause of overvoltages on distribution systems. Basically, lightning is a gigantic spark resulting from the development of millions of volts between clouds or between a cloud and the earth. It is similar to the dielectric breakdown of a huge capacitor. The voltage of a lightning stroke may start at hundreds of millions of volts between the cloud and earth. Although these values do not reach the earth, millions of volts can be delivered to the buildings, trees

or distribution lines struck. In the case of overhead distribution lines, it is not necessary that a stroke contact the line to produce overvoltages dangerous to equipment. This is so because "induced voltages" caused by the collapse of the electrostatic field with a nearby stroke may reach values as high as 300 kV [1].

Lightning is classified as a transient event. In order to understand the effect of lightning, it is best to acquire some knowledge as to what lightning is, how it is caused, and where it is most likely to occur [2]. The amount of energy contained in a lightning stroke is very high and it can be extremely destructive, even a single stroke to a distribution line can be sufficient to cause a blackout throughout a feeder.

Lightning is the main reason for outages in transmission and distribution lines [3]. When lightning strikes a power line, it is like closing a "big switch" between a large current source and the power line circuit. The sudden closing of this "big switch" causes an abrupt change in the circuit conditions, creating a transient. There is also the case when the lightning strikes the vicinity of the power line and the large magnetic field generated from the lightning current cause mutual coupling between the power line and the lightning. The event alters the conditions of the power line circuit, as a result, produce an electrical transient [4].

The study of lightning strokes in power lines is very important because it is known that lightning does strike the same structure over and again. This can be a very serious problem for power lines, typically, the highest structures located in high incidence lightning regions. Any structure, no matter its size, may be struck by lightning, but the probability of a structure been struck increases with its height [5]. Very close dart leaders can make as significant a contribution as return strokes in inducing voltages and currents on power systems [6].

## 2. Explanation of a Lightning

The duration of the lightning stroke is usually less than a couple of hundred microseconds as shown in Fig. 1. The industry accepted  $8 \times 20$  current wave shown in Fig. 1 as a reasonable approximation of a lightning surge [2].

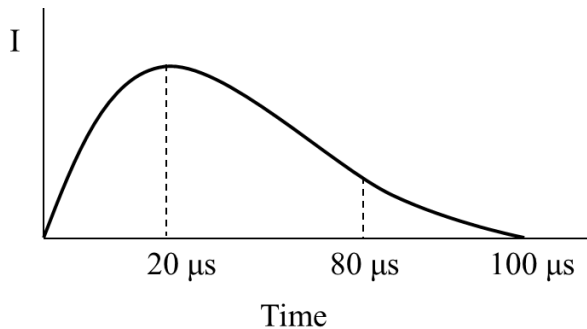


Fig. 1: Time duration of a typical lightning surge.

Cloud to ground flashes are composed of a single stroke or a multiple number of component strokes. Multiple stroke flashes have 3 to 4 strokes. The strokes are typically 40 to 50 ms apart. The typical lightning peak currents measured at ground range from 10 kA to 20 kA, but occasionally they range up to hundreds of thousands of amperes [5]. The peak current is reached in a few millionths of a second, and then it decreases in a thousandth of a second or so unless continuing current flows. Lightning flashes which contain continuing currents are called hot lightning. The continuing current lasts for one or two tenths of a second and has a typical peak value of 100 A. Hot lightning ignites fires. The lightning that does not contain a continuing current is called cold lightning and it does not set fires, but it is very destructive [5].

Lightning current magnitude is one of the most important lightning parameters, but the subject of lightning current magnitudes is controversial and confusing. Most experts agree that the stroke currents have been measured in excess of 200 kA, while almost all of the national and international standards on lightning protection are based on lightning current measurements made in Switzerland and usually described by the median value and standard deviation or by 5, 50, and 95 % values as shown in Tab. 1 [7].

Tab. 1: Lightning current magnitudes.

Lightning current distribution statistics			
	95 %	50 %	5 %
Negative first strokes [kA]	14	30	80
Negative subsequent strokes [kA]	4,6	12	30

## 3. Lightning Prevention

Lightning rods are used as prevention mechanisms to avoid lightning hitting tall buildings or houses where lightning incidence is high, but no lightning rod can offer absolute protection [5]. A lightning rod protection system has three main parts:

- The rods on the top of the protected structure.
- The wires which connect the rods together and those which run down the sides of the structure to the grounding arrangement.
- The grounding arrangement.

To protect high voltage transmission lines from lightning, the metallic rods and wire conductors are replaced by a system of wires suspended between tall towers arranged around the structure. These grounded wires are strung above the high voltage lines to intercept strokes that would otherwise hit the power lines [5].

If a lightning stroke hits a power line, the only way to protect it is using a lightning arrester (LA). The lightning arrester is a non-linear device that acts as an open circuit to low potentials, but conducts electrical current at very high potentials. When lightning strikes a line protected with a lightning arrester, the non-linear resistance draws the current to ground. One of the most common lightning arresters is the MOV (Metal Oxide Varistor) [8]. The MOV has a piece of metal oxide that is joined to the power and grounding line by a pair of semiconductors. The semiconductors have a variable resistance dependent on voltage. When the voltage level in the power line is at the rated voltage for the arrester, the electrons in the semiconductors flow in a way that creates a very high resistance. If the voltage level in the power line exceeds the arrester rated voltage, the electrons behave differently and create a low resistance path that conducts the injected lightning current to the ground system.

## 4. Types of Surge Arresters

Surge arresters used for protection of exterior electrical distribution lines will be either of the Metal-Oxide Surge Arrester (MOSA), with resistors made of zinc-oxide (ZnO) blocks, or gapped type with resistors made of Silicon-Carbide (SiC). Expulsion type units are no longer used.

Metal-oxide (MO) surge arresters are widely used as protective devices against switching and lightning over-voltages in power systems. The distinctive features of the MO arresters are their extremely non-linear

voltage-current or V-I characteristic, ignorable power losses, high level reliability in the operation time, high speed response to the over-voltages, simplicity of design, easier for maintenance and long life time. Accurate modeling and simulation of their dynamic characteristics are very important for arrester allocation, systems reliability and insulation coordination studies [9], [10], [11]. For switching over voltages studies, the surge arresters can be represented by their nonlinear V-I characteristics (or U-I characteristics). However, such a presentation would not be suitable for fast front transient and lightning surge studies. Because the MO surge arrester exhibits dynamic characteristics such that the voltage across the surge arrester increases as the time-to-crest of the arrester current decreases and the voltage of arrester reaches a peak before the arrester current peaks [9]. Typically, the residual voltage for an impulse current having a front time equal to  $1 \mu\text{s}$  is 8–12 % higher than that of predicted for an impulse current having a front time equal to  $8 \mu\text{s}$ . The residual voltage for longer time-to-crests between 45 and  $60 \mu\text{s}$ , is 2–4 % lower than that of a  $8 \mu\text{s}$  current impulse [11]. In order to reproduce the MO surge arrester dynamic characteristics mentioned previously, a lot of researches have been done on modeling and simulation of MO surge arresters [11]. A dynamic model has been presented based on the data base of [9] for fast impulse currents (time-to-crest of  $0,5\text{--}4,5 \mu\text{s}$ ). To estimate the model parameters, an iterative trial and error procedure has been proposed, which matches the peak of discharge voltage obtained with  $8 \times 20 \mu\text{s}$  impulse current.

## 5. Surge Arrester Models

The IEEE WG 3.4.11 group proposed the model shown in Tab. 2 (IEEE model). This model includes the nonlinear resistors, designated by  $A_0$  and  $A_1$ , separated by RL low pass filter [9], where their parameters are calculated from the estimated height of the arrester, the number of columns of MO disks and the curves shown in Fig. 2.

The model in Tab. 2 (Pinceti model) has been proposed by Pinceti-Gianettoni [10]. This model is based on IEEE model with some differences. The capacitance is eliminated, since its effect on model behavior is negligible. Resistance  $R$  (about  $1 \text{ M}\Omega$ ) replaced between the input terminals, only to avoid numerical troubles. Resistance  $R_0$  stabilizes the numerical oscillations and the nonlinear resistors  $A_0$  and  $A_1$  can be estimated by using the curves shown in Fig. 2.

The model proposed by Fernandez-Diaz [12], shown in Tab. 2 (Fernandez-Diaz model), has recently been developed which is recommended by IEEE W.G. 3.4.11 and Pinceti model. The non linear resistors  $A_0$  and  $A_1$

are connected in parallel and separated by inductance  $L_1$ . Capacitance  $C$  is the value of terminal to terminal of capacitor and the resistor represents of arrester which has the value of the whole resistance of  $1 \text{ M}\Omega$ .

Other models are developed and simplified such as a Popov model for switching studies, and its parameters can be estimated by an iterative trial and error procedure, proposed in [13], and a CIGRE model [14].

## 6. Parameters of $A_0$ and $A_1$

To define non-linear parameter resistors,  $A_0$  and  $A_1$  the reference from the committee of IEEE W.G. 3.4.11 is used. The experiments obtain the characteristic curves of current and voltage of both non-linear resistors as shown in the curves in Fig. 2 [10] or in Tab. 3 below [9].

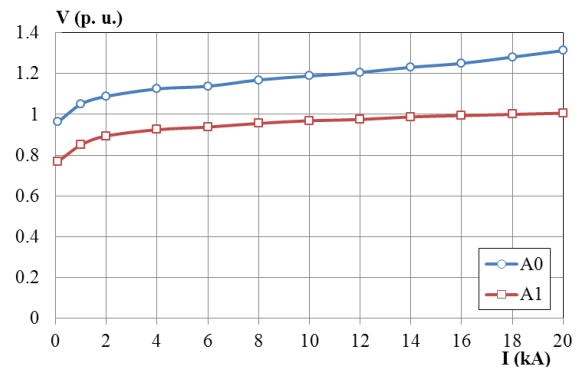


Fig. 2: V-I characteristics of nonlinear  $A_0$  and  $A_1$ .

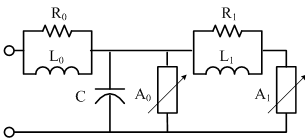
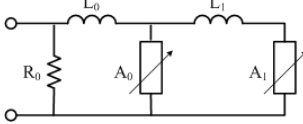
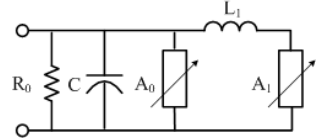
Tab. 3: V-I characteristics for  $A_0$  and  $A_1$ .

I [kA]	V [p.u]	
	$A_0$	$A_1$
0,1	0,963	0,769
1	1,05	0,85
2	1,088	0,894
4	1,125	0,925
6	1,138	0,938
8	1,169	0,956
10	1,188	0,969
12	1,206	0,975
14	1,231	0,988
16	1,25	0,994
18	1,281	1
20	1,313	1,006

## 7. A Conventional Model

The ATP-Draw offers a metal oxide arrester with MOV Type-92 component. If this component is specified, ATP-Draw accepts the current-voltage characteristic

Tab. 2: Arrester models.

IEEE model	Pinceti model	Fernandez-Diaz model
 <p> <math>L_1 = 15d/n</math> [<math>\mu\text{H}</math>]  <math>R_1 = 65d/n</math> [<math>\Omega</math>]  <math>L_0 = 0,2d/n</math> [<math>\mu\text{H}</math>]  <math>R_0 = 100d/n</math> [<math>\Omega</math>]  <math>C = 100n/d</math> [<math>\text{pF}</math>]  <math>d</math> is the estimated height of the arrester in meter  <math>n</math> is the number of parallel columns of MO in the arrester                 </p>	 <p> <math>L_1 = \frac{1}{4} \frac{U_{r1/T2} - U_{r8/T2}}{U_{r8/T2}} U_r</math> [<math>\mu\text{H}</math>]  <math>L_0 = \frac{1}{12} \frac{U_{r1/T2} - U_{r8/T2}}{U_{r8/T2}} U_r</math> [<math>\mu\text{H}</math>]  <math>U_r</math> is the rated voltage  <math>U_{r1/T2}</math> is the residual voltage at 10 kA fast front current surge (1/T2 <math>\mu\text{s}</math>)  <math>U_{r8/20}</math> is the residual voltage at 10 kA current surge with 8/20 <math>\mu\text{s}</math> shape  <math>R_0 = 1 \text{ M}\Omega</math> is introduced to avoid numerical instabilities                 </p>	 <p> <math>L_1 = \frac{2}{5} \frac{U_{r8/T2} - U_{ss}}{U_{r8/T2}} U_r</math> [<math>\mu\text{H}</math>]  <math>C = \frac{1}{55} \frac{U_{r8/T2} - U_{ss}}{U_{r8/T2}} U_r</math> [<math>\text{pF}</math>]  <math>U_r</math> is the rated voltage  <math>U_{r8/20}</math> is the residual voltage at 10 kA current surge with 8/20 <math>\mu\text{s}</math> shape in kV  <math>U_{ss}</math> is the residual voltage at 500 A current surge switching 60/2000 <math>\mu\text{s}</math> or 30/70 <math>\mu\text{s}</math> in kV  <math>R_0 = 1 \text{ M}\Omega</math> </p>

and performs an exponential fitting in the log-log domain to produce the required ATP data format. In this paper, the surge arrester conventional model was represented by a nonlinear resistor (model Type-92 from ATP). This model provides a true representation of the nonlinearity of the varistor through a piecewise-linear characteristic of current and voltage [15]. In this model, the dynamic characteristic of the surge arrester is not taken into account. The voltage peak occurs in the same time of current peak, even for current waveforms which the peak is in the range of 8  $\mu\text{s}$  and faster.

### 8. Test System

For the simulation of the impact of lightning strikes on electric power systems, a test system was assembled by ATP-Draw version 4.2p1. The system, Fig. 3, corresponds to a part of a power network 22 kV fed from the supply network 110 kV with a short-circuit power  $S_k = 1500 \text{ MVA}$  via the transformer T1. The main transmission line1 is about 60 km long and the branches lengths are as shown in Fig. 3 below. The lightning flash was based on the cold lightning flash and it is composed of three sequential spikes with different magnitudes. The first stroke is about 10 kA with duration of 0,6 ms, the second subsequent stroke has a magnitude of 5 kA and the third of 3 kA and both with duration of 0,3 ms.

### 9. ATP-Draw Modeling

The supply network is represented by the source of voltage with amplitude equals to Eq. (3) [14] and it's internal impedance ( $R = 0,803 \Omega$ ,  $L = 25,56 \text{ mH}$ ) calculated from the short-circuit power  $S_k$ . The model of the supply network by ATP-Draw was AC3ph-Type 14 (Steady-state (cosinus) function 3 phase).

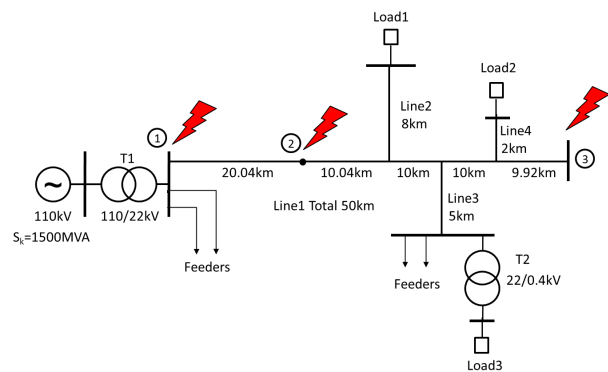


Fig. 3: Scheme of the power network.

$$U_{amp} = \frac{\sqrt{2}}{\sqrt{3}} \cdot 100 = 89,804 \text{ kV.} \tag{1}$$

The transformers are modeled by the ATP-Draw model BCTRAN. Table 4 describes the parameters of the transformers.

Tab. 4: Parameters of BCTRAN.

Transformer	T1	T2
Power [MVA]	16	0,4
Primary voltage [kV]	110	22
Secondary voltage [kV]	23	0,42
Short-circuit voltage [%]	11,53	4
Open-circuit current [%]	0,22	1,1
Short-circuit losses [kW]	62,7	4,6
Open-circuit losses [kW]	15,2	0,65
No. of windings	2	2

The other values: number of phases: 3, shell core, test frequency 50 Hz and the connection is Ynyn (voltage divided by  $\sqrt{3}$ ).

- The transmission lines 22 kV are made of AlFe<sub>6</sub> and all are modeled by LCC Lines/Cables procedure as an overhead line, 3phase with PI-Model.

Ground resistivity  $\rho = 20 \Omega\text{m}$ , Freq. init = 50 Hz. The parameters are in Tab. 5 and the placement of the conductors as shown in Fig. 4. The simulation was done with the assumption that the placement of the conductors on the tower for all lines is (1,75, 0,4, -1,75 and for ground -0,09),  $V_{tower} = 10,25$  m and  $V_{mid} = 10$  m.

Tab. 5: The parameters of the transmission lines.

Line	Section area [mm <sup>2</sup> ]	Rout [cm]	Resis [ $\Omega \cdot \text{km}^{-1}$ ]	React [ $\Omega \cdot \text{km}^{-1}$ ]
1	185	0,95	0,1773	0,3272
2	120	0,8	0,234	0,421
3	95	0,675	0,319	0,430
Ground	35	0,42	0,778	0,428

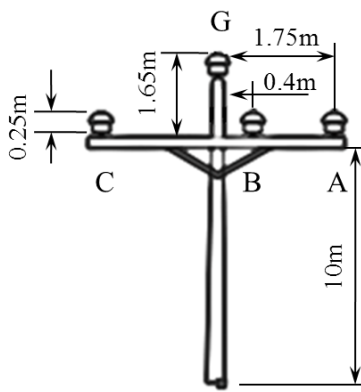


Fig. 4: Dimensions of the tower.

- Loads 1 and 2 are equivalent to industrial loads, where load1 is about 4,5 MW, 2,5 MVar and load 2 is about 3,8 MW, 2 MVar. Assuming that the transformer T2 is full loaded, the power factor is 0,95 and load 2 is consisting in a load of some residential areas and was measured as 0,380 MW, 0,120 MVar. Load is modeled by the standard component RLC\_3. The parameters are calculated as following [16] without C, and the values are listed in Tab. 6.

$$R = \frac{U^2}{P} \tag{2}$$

$$L = \frac{U^2/Q}{2\pi f} \tag{3}$$

Tab. 6: The parameters of the transmission lines.

Load	U [kV]	P [MW]	Q [MVar]	R [ $\Omega$ ]	L [mH]
1	22	4,5	2,5	107,556	616,561
2	22	3,8	2	127,369	770,701
3	0,4	0,380	0,120	0,421	4,2463

- The lightning flash is implemented in ATP-Draw using three shunt connected ideal current sources. The first stroke, represented in Fig. 5, was simulated using a Type-15 surge function [17]. This function is suitable and given by:

$$f(t) = \text{amplitude} (e^{At} - e^{Bt}) \tag{4}$$

The constants amplitude,  $A$  and  $B$  were selected to provide a surge value of 10 kA for the duration of 0,6 ms. Constants values are presented in Tab. 7.

Tab. 7: The surge function values.

Amplitude [A]	A [ $\text{l}\cdot\text{s}^{-1}$ ]	B [ $\text{l}\cdot\text{s}^{-1}$ ]	T-start [s]	T-stop [s]
16000	-8500	-60000	0	0,0006

The second and third strokes were simulated by Type-13 ramp functions of 0,3 ms duration with 5 kA and 3 kA amplitude, respectively. The values for the functions are listed in Tab. 8. Figure 6 shows the simulated lightning flash as simulated in ATP-Draw.

Tab. 8: The ramp function values.

Stroke	1	2
Amplitude [A]	5000	3000
T0 [s]	0	0
A1 [A]	0	0
T1 [s]	0,0003	0,0003
T-start [s]	0,06	0,03
T-stop [s]	0,0603	0,1203

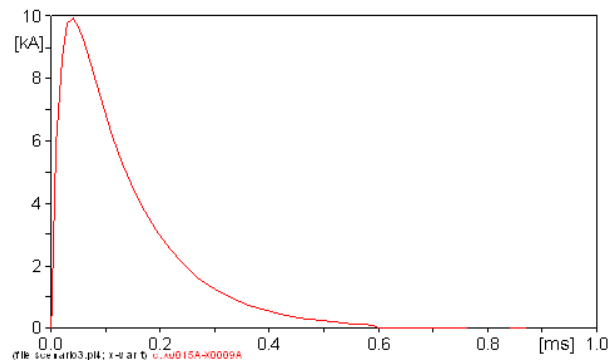


Fig. 5: The first lightning stroke (20 kA, 0,6 ms).

- Lightning arrester is modeled by MOV-Type 92 component [15]. The used lightning arrester was identical ABB Surge arrester POLIM-D, distribution class heavy duty, designed and tested according to IEC 60099-4. The thermal stability of the MO-surge arrester is proved in the operating duty test with the application of one high current impulse  $I_{hc} = 100$  kA, which gives an energy input of 3,6 kJ/kV ( $U_c$ ) and its characteristics were taken from manufacturer datasheets [18]. Arrester residual voltage curve is shown in Fig. 7.

Tab. 9: Aresster characteristics.

Max. continous operating voltage $U_c$ (kVcrest)	22				
Rated Voltage $U_r$ kV (rms)	27,5				
Residual voltage ( $U_{res}$ ) in kV (crest) at specified discharge current (crest) wave 8/20 $\mu$ s	1 kA	2,5 kA	5 kA	10 kA	20 kA
	64	67,8	71,7	77	87,4
Temporary overvoltage (TOV) $U_{TOV}$	$t = 1$ s, $U_{TOV} = 1,325 \times U_c$ $t = 3$ s, $U_{TOV} = 1,300 \times U_c$ $t = 10$ s, $U_{TOV} = 1,275 \times U_c$				

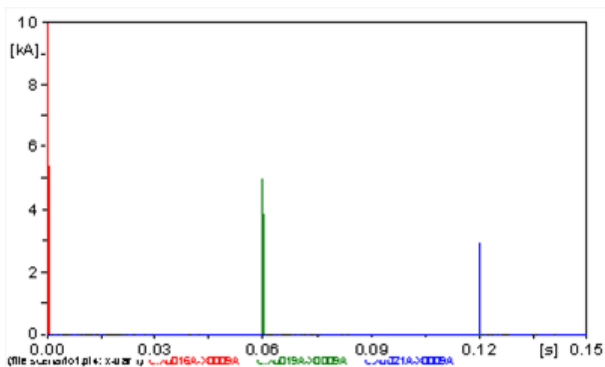


Fig. 6: The lightning flash as simulated in ATP-Draw.

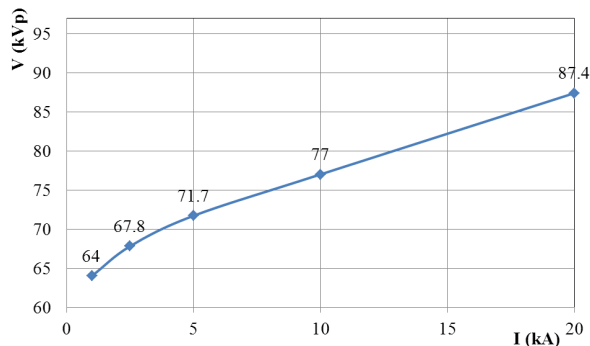


Fig. 7: Arrester residual voltage curve.

- Lightning hits the phase A at the middle distance between the transmission towers, about 20,04 km far from the substation 110/22 kV.
- Lightning hits the phase A at the far end of the main transmission line 1.

The two line end cases were simulated to investigate the effects of a lightning strike directly to the loads, while the centre case was simulated to assess the propagation of the induced lightning surge across the line. The ATP scheme of the power network is shown in Fig. 8 below for scenario 1.

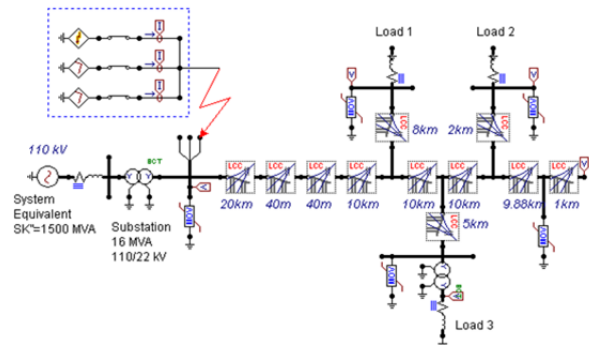


Fig. 8: ATP scheme of the power network (scenario 1).

## 10. Simulation Results and Discussion

In this study two different cases will be analysed, case with no lightning arresters installed and another with them. Case 1 has three scenarios of contact locations marked as 1, 2 and 3 described as follows, while case 2 will be applied just for the worst scenario that may occur in the simulation:

- Lightning hits the phase A at the substation 110/22 kV - secondary side.

### 10.1. Case 1

As expected, the impact is destructive for cases without lightning arresters. The severity is enough to guarantee insulation failure on line structures and damage to connected equipment. The voltage waveforms after the lightning are shown in the figures below for phase A and for the three scenarios (waveforms are overlapping on each other). The maximum recorded voltages, caused by only the first strike, are listed in Tab. 10.

It is notable from the above results, that the voltages induced by the first stroke can reach values of the order

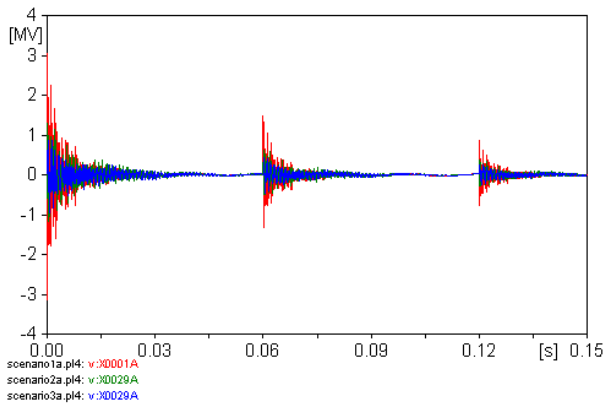


Fig. 9: Voltages at substation 110/22 kV for the three scenarios.

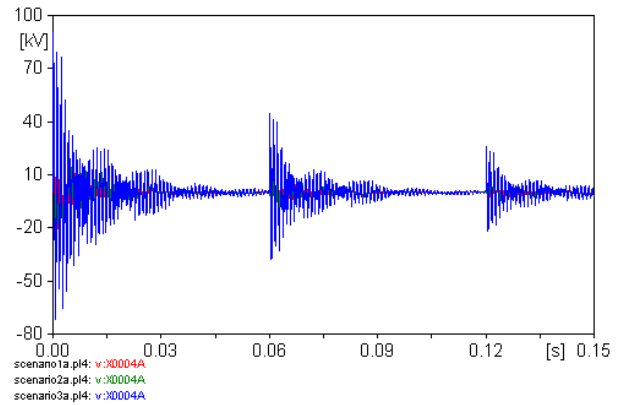


Fig. 12: Voltages at load 3 (sec. side) for the three scenarios.

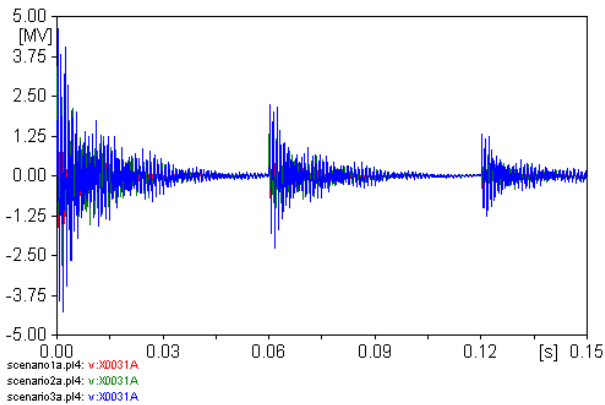


Fig. 10: Voltages at load 1 for the three scenarios.

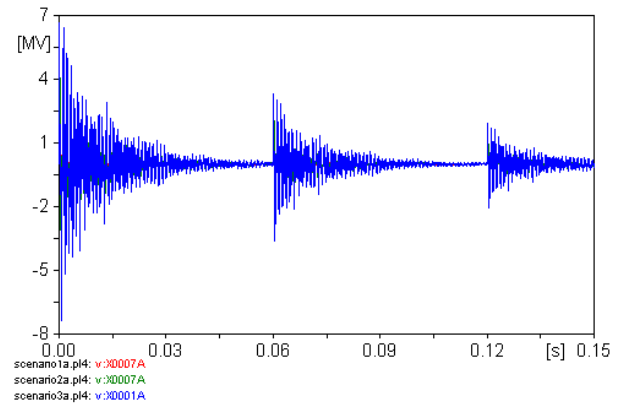


Fig. 13: Voltages at the end point of line 1 for the three scenarios.

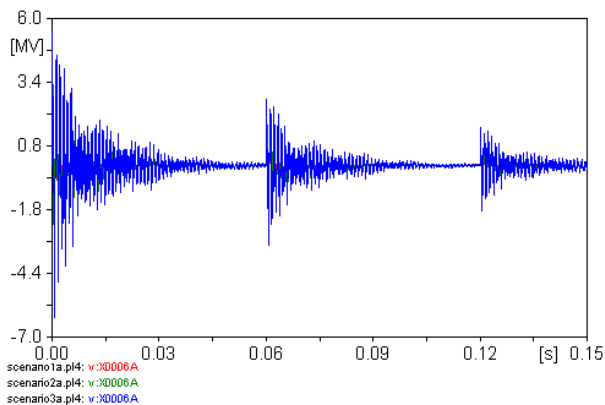


Fig. 11: Voltages at load 2 for the three scenarios.

Tab. 10: Maximum voltages caused by the first strike.

Place	Max. voltage [kV]		
	scenario 1	scenario 2	scenario 3
Substation 110/22 kV	3050,3	1281,2	1518
Load 1	1566,5	3431,5	4614,5
Load 2	1142,8	3287,3	5442,5
Load 3 (sec. side)	24,632	53,065	90,538
End of line 1	1516	4083,5	6644,9
Point of impact	-	3172	-

of millions. Maximum registered voltages at the network for the three scenarios are clearly over insulation flashover levels for 22 kV equipment (22 kV/150 kV BIL, 110 kV/550 kV BIL). The basic impulse level (BIL) of the transformer measures its ability to withstand these surges [1].

It should be taken into consideration one interesting detail, reflections along the feeder are able to amplify the surge, thereby, producing higher voltages into the feeder. That can be seen from Tab. 10, where the max-

imum voltages, in comparison with the point of impact, are recorded in the other ends of the line.

### 10.2. Case 2

In such study it is intended to include lightning arrester installations to avoid the destructive effects of lightning. Referring to the results in Tab. 10, scenario 3 produced the maximum voltages and the figures after lightning arrester installations will be shown just for this scenario, also Tab. 11 shows the changes of the

results, shown in Tab. 10 for this scenario, after using lightning arrester.

Determining the optimum locations for transmission line arresters is not a simple task. If no arresters are installed on a line, it is a well known fact that with a direct strike to a phase conductor, there is a 100 % probability of an insulator flashover. It is also a fact that if arresters are installed on every phase of every tower, a direct strike to the shield or phase conductor will result in 0 % probability of an insulator flashover [18].

After several tries of simulations, lightning arresters in the substation 110/22 kV, all loads and one LA about 1 km far from the end point of line 1 were installed as shown in Fig. 8. The results of the simulation are as follows:

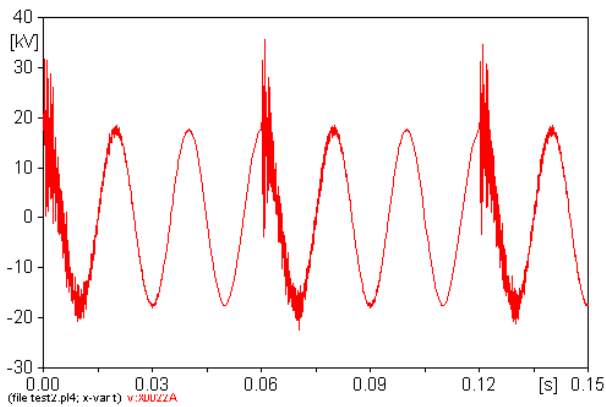


Fig. 14: Voltage at substation 110/22 kV with arresters.

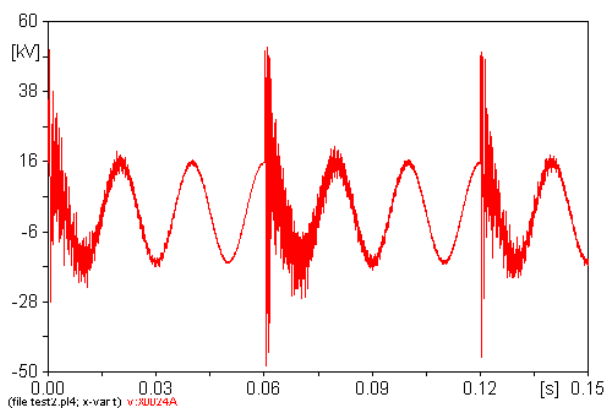


Fig. 15: Voltage at load 1 with arresters.

The results give a clear view of the lightning arresters ability to immediately reduce lightning impact on the power system. All figures show greatly decreased voltage peaks, but it must be taken into consideration that these results depend on the placement of the lightning arresters across the network as described previously.

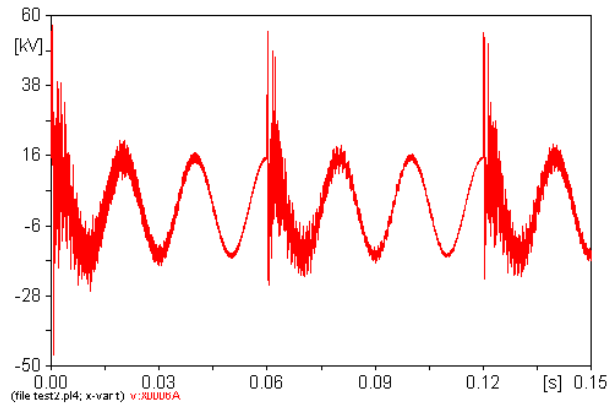


Fig. 16: Voltage at load 2 with arresters.

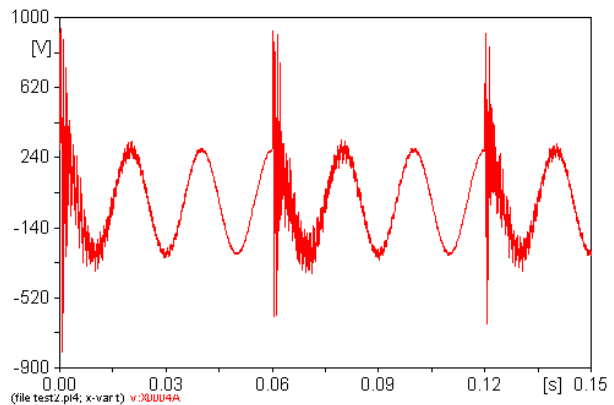


Fig. 17: Voltage at load 3 with arresters.

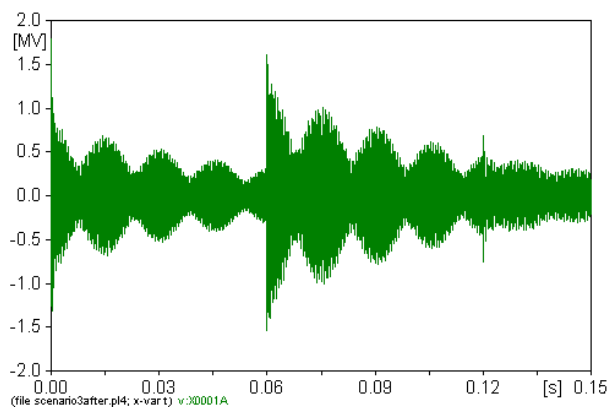


Fig. 18: Voltage at the point of impact with arresters.

Tab. 11: Maximum voltages after using lightning arrester.

Place	Max. voltage [kV]
	scenario 3
Substation 110/22 kV	35,69
Load 1	52,024
Load 2	56,77
Load 3 (sec. side)	0,939
End of line 1 (Point of impact)	1796,1



All values are within flashover and BIL ratings of the network equipment (22 kV/150 kV BIL). However, voltage magnitude at the point of the lightning contact is still of astronomical proportions (namely 1,796 MV, see Fig. 18). Magnitudes of this proportion are still able to cause flashover and surely the destruction of the adjacent distribution poles [4].

Energy dissipated by the arresters is shown in Fig. 19 and Fig. 20. As is illustrated in Fig. 19, maximum dissipated energy reached the value 2,9 kJ at load 2. This value is within the maximum allowable energy dissipation for the arrester model, namely 79,2 kJ (max. 3,6 kJ/kV ( $U_c$ ) where  $U_c = 22$  kV). A point of concern though, is the energy dissipation of the arrester close to the point of impact. The curve shown at Fig. 20 illustrates that the first stroke will cause arrester failure, where the maximum dissipated energy reached 114,07 kJ. Because of this, if such an event could happen in the power system, higher energy class arresters are required, otherwise, the arresters must be replaced after such events.

Choosing an arrester rating for a distribution system is based on the system's line-to-ground voltage and the way it is grounded [1]. The limiting condition for an arrester does not usually have anything to do with the magnitude of the surges (switching or lightning) that it might see. This is in contrast to the selection of arresters for transmission.

An arrester usually has a limited protective zone of only a few meters to up to several ten meters, where the protective zone is defined as the maximum separation distance for which the insulation coordination requirements are fulfilled for a given arrester protective level and coordination withstand voltage (IEC 60099-5, sub-clause 4.3.1). Arresters, therefore, should be installed as close as possible to the device to be protected.

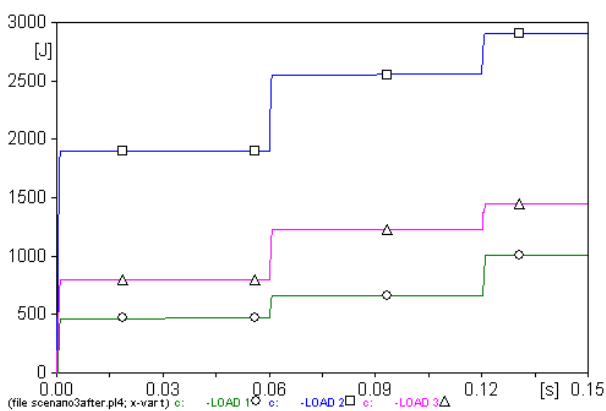


Fig. 19: Dissipated energy at loads.

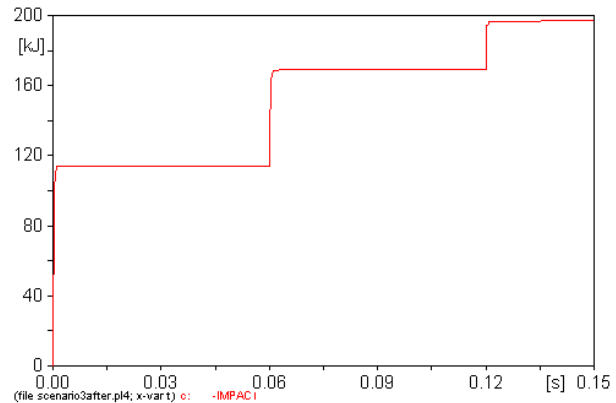


Fig. 20: Dissipated energy close to the point of impact.

## 11. Conclusion

In this paper, the effects of a lightning strike is simulated and analyzed by the ATP-Draw. A multiple stroke lightning flash was successfully simulated in ATP by using surge function and ramp functions. The lightning was used to investigate the impact of such transient phenomena in power systems.

Results obtained by this study, show how dangerous the lightning on electrical systems is. The voltages induced by the lightning reached values of the order of MV (see Tab. 10), which are clearly over insulation flashover levels for 22 kV equipment (22 kV/150 kV BIL). That is very detrimental for system performance and exposes loads and devices to unnecessary overvoltages which may cause insulation flashovers and device failures.

The results establish the need for lightning protection by using lightning arresters. The lightning arrester was represented by the ATP MOV-Type 92 component. This conventional model cannot represent the capacitive behavior (only the resistive behavior) of the MOSA, which occurs whenever it is excited by a voltage below of the rated voltage. Therefore the results of energy absorption at voltage operation were divergent. Nevertheless such study can be made to identify a different arrester model more suitable for the power systems.

## References

- [1] BEATY, H. W. *Standard Handbook for Electrical Engineers*. New York: McGraw-Hill Professional, 2006. ISBN 978-0071762328.
- [2] BURKE, J. J. *Power Distribution Engineering—Fundamentals and applications*. New York: CRC Press, 1994. ISBN 978-0824792374.

- [3] GREENWOOD, A. *Electrical Transients in Power Systems*. New York: John Wiley & Sons, 1991. ISBN 978-0471620587.
- [4] RODRIGUEZ-SANABRIA, D. and C. RAMOS-ROBLES. Lightning and Lightning Arrester Simulation in Electrical Power Distribution Systems. In: *Electrical and Computer Engineering: University of Puerto Rico* [online]. 2005. Available at: [http://ece.uprm.edu/~lorama/Proy\\_Rayos03.pdf](http://ece.uprm.edu/~lorama/Proy_Rayos03.pdf).
- [5] UMAN, M. A. *All About Lightning*. Toronto: Dover Publications, 1986. ISBN 978-0486252377.
- [6] RAKOV, V. A., M. A. UMAN, K. J. RAMBO, M. I. FERNANDEZ, R. J. FISCHER, G. H. SCHNETZER, R. THOTTAPPILLIL, A. EYBERT-BERARD, J. P. BERLANDIS, P. LALANDE, A. BONAMY, P. LAROCHE and A. BONDIOU-CLERGERIE. New Insights into Lightning Processes from Triggered-Lightning Experiments in Florida and Alabama. *Journal of Geophysical Research*. 1998, vol. 103, no. D12, pp. 14117–14130. ISSN 2156-220.
- [7] DIENDORFER G., W. SCHULZ and V. A. RAKOV. Lightning Characteristics Based on Data from the Austrian Lightning Locating System. *IEEE Transactions on Electromagnetic Compatibility*. 1998, vol. 40, iss. 4, pp. 452–464. ISSN 0018-9375. DOI: 10.1109/15.736206.
- [8] MACKEVICH, J. P. Proper Lightning Arrester Application Improves Distribution System Reliability. In: *2nd International Conference on Advances in Power System Control, Operation and Management, 1993. APSCOM-93*. Hong Kong: IEEE, 1993, pp. 153–158. ISBN 0-85296-569-9.
- [9] IEEE Working Group 3.4.11. Modeling of metal oxide surge arresters. *IEEE Transactions on Power Delivery*. 1992, vol. 7, iss. 1, pp. 302–309. ISSN 0885-8977. DOI: 10.1109/61.108922.
- [10] PINCETI, P. and M. GIANNETTONI. A simplified model for zinc oxide surge arresters. *IEEE Transactions on Power Delivery*. 1999, vol. 14, iss. 2, pp. 393–398. ISSN 0885-8977. DOI: 10.1109/61.754079.
- [11] MARTINEZ, J. A. and D. W. DURBAK. Parameter determination for modeling systems transients-part V: Surge arrester. *Transactions on Power Delivery*. 2005, vol. 20, iss. 3, pp. 2073–2078. ISSN 0885-8977. DOI: 10.1109/TPWRD.2005.848771.
- [12] FERNANDEZ, F. and R. DIAZ. Metal oxide surge arrester model for fast transient simulations. In: *International Conference on Power System Transients IPST01*. Rio De Janeiro: Federal University of Rio de Janeiro, 2001, pp. 144-1–144-5.
- [13] POPOV M., L. SLUIS and G. C. PAAP. Application of a new surge arrester model in protection studies concerning switching surges. *IEEE Power Engineering Review*. 2002, vol. 22, iss. 9, pp. 52–53. ISSN 0272-1724. DOI: 10.1109/MPER.2002.4312562.
- [14] THANASAKSIRI, T., S. PREMRUDEEP-REECHACHAN, W. TAYATI and P. JIRAPONG. Improving the Lightning Performance of Overhead Distribution Lines in Thailand Using Lightning Protection Design Workstation (LPDW). In: *Proceedings of the IASTED International Conference, PowerCon 2003 (Special Theme: BLACKOUT)*. New York: Acta Press, 2003, pp. 39–48. ISBN 978-0889864009.
- [15] Leuven EMTP Center. *Alternative Transients Program: Rule Book*. Heverlee: EMTP, 1987.
- [16] MIKULEC M. and V. HAVLICEK. *Fundamentals of electromagnetic circuits 1*. Prague: CVUT, 1997. ISBN 80-01-01620-X.
- [17] PRIKLER, L. and H. K. HOIDALEN. *ATPDraw version 5.6 for windows 9x/NT/2000/XP/Vista: Users Manual*. 2002. Available at: <http://www.elkraft.ntnu.no/atpdraw/ATPDMan56.pdf>.
- [18] High Voltage Products: Surge Arrester. In: *ABB Switzerland Ltd.* [online]. 2013. Available at: <http://www.abb.com/product/us/9AAC710009.aspx>.

## About Authors

**Shehab Abdulwadood ALI** was born in Aden 1965. He obtained his M.Sc. and Ph.D. degrees in the field of Electrical Power Engineering from VSB–Technical University of Ostrava, Czech Republic. He was appointed as Associate Professor at Faculty of Saber of Aden University. Currently he acts as a lecturer in electricity and electronics. Interests are power quality and electromagnetic compatibility problems with using ATPDraw and NetCalc.